

ESTIMATING SCALING EXPONENTS IN AUDITORY-NERVE SPIKE TRAINS USING FRACTAL MODELS INCORPORATING REFRACTORINESS

S.B. LOWEN

*Department of Electrical and Computer Engineering
44 Cummington Street
Boston University, Boston, MA 02215
lowen@bu.edu*

M.C. TEICH

*Department of Electrical and Computer Engineering
Department of Biomedical Engineering
44 Cummington Street
Boston University, Boston, MA 02215
teich@bu.edu*

Fractal stochastic point processes (FSPPs) provide good mathematical models for long-term correlations present in auditory-nerve fibers in a number of species. Simulations and analytical results for FSPPs concur with experimental data over long times. Refractoriness-modified Poisson point processes, in contrast, model only the short-term characteristics of these data. FSPPs incorporating refractoriness yield superior results over all time scales, and analytical results for the statistics of this model agree closely with both computer simulations and auditory data. Furthermore, these processes provide a superior method for estimating the fractal exponent α , which parametrizes the long-term correlation found in these recordings.

1 Introduction

Certain random phenomena are well described by essentially identical events occurring at discrete times. One example is the registration of action potentials recorded by an electrode near an auditory-nerve fiber^{3,16,17}. A (one-dimensional) stochastic point process is a mathematical construction which represents these events as random points on a line. Such a process may be called fractal when a number of the relevant statistics exhibit scaling with related scaling exponents, indicating that the represented phenomenon contains clusters of points over a relatively large set of time scales^{11,5,6,7}.

The power spectral density (PSD) and the Allan factor (AF) are two statistics which reveal this clustering^{7,9,1}. The PSD $S(\omega)$ for a point process, as for continuous-time processes, provides a measure of how power is concentrated as a function of the angular frequency ω . The Allan factor $A(T)$, is defined as the ratio of the Allan variance of the event count in a specified time window

T to twice the mean count. The Allan variance, in turn, is the variance of the *difference* between the numbers of counts in adjacent windows of duration T . For an FSPP, over a large range of times and frequencies, it can be shown that^{7,9,1}

$$\begin{aligned} \text{PSD: } S(\omega)/\lambda &\approx 1 + (\omega/\omega_0)^{-\alpha} \\ \text{AF: } A(T) &\approx 1 + (T/T_0)^\alpha, \end{aligned} \quad (1)$$

with λ the average rate of the process, $\alpha > 0$ the fractal exponent, ω_0 a cutoff frequency, T_0 a cutoff time, and $\omega_0^\alpha T_0^\alpha = (2 - 2^\alpha) \cos(\pi\alpha/2) \Gamma(\alpha + 2)$ ^{9,10}. Thus in this mathematical formalism, the fractal exponent α can assume values in excess of unity, as sometimes occurs in auditory recordings⁹.

The homogeneous Poisson point process (HPP) is perhaps the simplest stochastic point process, being fully characterized by a single constant quantity, its rate. It is not fractal, but serves as a building block for other point processes which can be. With the inclusion of refractoriness (dead- and sick-time effects), the refractoriness-modified Poisson point process (RM-P)^{14,12,15} proves successful in modeling auditory-nerve spike trains over short time scales. With fixed and exponentially distributed²⁰ random refractoriness together¹⁵, the RM-P predicts an interevent-interval histogram (IIH) of the form

$$p(t) = \begin{cases} \lambda(1 - \lambda r)^{-1} \{ \exp[-\lambda(t - f)] - \exp[-(t - f)/r] \} & \text{for } t > f \\ 0 & \text{for } t \leq f. \end{cases} \quad (2)$$

where λ is the original rate of events (before refractory effects), f is the portion of the refractory period that is fixed, and r is the mean of the random component.

However, the accurate modeling of the self-similar or fractal behavior observed in sensory-system neural spike trains over long times requires a fractal stochastic point process^{16,13,17,4,18,2,9}. A number of FSPP models have been developed⁷; we focus on a particular process, the fractal-Gaussian-noise-driven Poisson process (FGNDP)⁷. The FGNDP is important because Gaussian processes are ubiquitous, well understood, and are completely described by their means and autocovariance functions. Thus only three parameters (including the rate) are required to specify an FGNDP, since, like all FSPPs, it follows Eq. 1. The FGNDP describes the firing patterns of primary auditory afferents quite well over long time scales (several hundred milliseconds and larger)¹⁷, although it does not accurately model neural activity over short time scales. Therefore procedures for estimating the fractal exponent α based on a simple FSPP formalism that ignores refractoriness, such as a least-squares fit to the logarithm of Eq. 1, necessarily yield biased results. The parameter α plays a crucial role in characterizing the auditory-nerve fiber recordings, since this

single quantity describes the long-term correlations present in such recordings, and the singularity near zero frequency in the PSD⁹.

2 Models Incorporating Refractoriness and Fractal Behavior

Incorporating refractory effects into the fractal behavior of the FGNDP yields the refractoriness-modified version (RM-FGNDP), a new model which does indeed mimic auditory-nerve behavior over all time and frequency scales⁸. Figure 1 shows the AF obtained from a recording of an auditory-nerve fiber under spontaneous conditions (solid curve), and from a single simulation of the RM-FGNDP process (dashed curve). All recordings used in this paper were obtained from one cat auditory afferent fiber, with a spontaneous rate of 75 spikes/sec, and a characteristic frequency (CF) of 3926 Hz. (Data collection and minimal subsequent processing methods are described in Ref. 9 and references therein.) The two curves agree within the limits imposed by fluctuations inherent in a finite data length; agreement also obtains for other statistics such as the IHH, not shown. Evidently, simulations of the RM-FGNDP process mimic auditory-nerve-fiber data well. Simulations of non-fractal models, in contrast, exhibit AF curves which never exceed unity, and thus are not suitable as models of auditory-nerve firing behavior. Conversely, simulations of

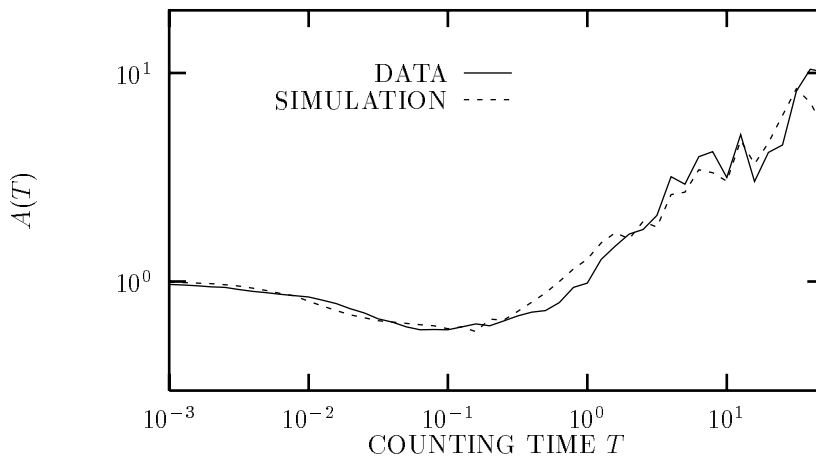


Figure 1: Doubly logarithmic plot of the Allan factor (AF) for auditory-nerve-fiber data recorded under spontaneous conditions (solid curve), and for a simulation of the RM-FGNDP process with parameters chosen to fit the data (dashed curve).

non-refractory models exhibit AF curves which never dip below unity, while those of the data always do.

Fortuitously, for the parameter ranges employed in modeling these spike trains, the effects of the fractal fluctuations are minimal over the time scales where refractoriness dominates, and vice versa; thus these two effects may be decoupled in the modeling procedure. In particular, the IIH plots for the full RM-FGNDP theory, the non-fractal RM-P models, and the data all resemble each other closely.

The AF and PSD for the RM-FGNDP, in contrast, do differ appreciably from those of both the (non-fractal) RM-P and (non-refractory) FGNDP models. We have developed new analytical formulas for these quantities in the presence of generalized refractoriness (including both fixed and exponentially distributed random components)¹⁰, and provide two key results below. For steady-state (equilibrium) counting¹², and for $T \gg f, r$, the AF assumes the form, over all counting times:

$$A(T) \approx \frac{6a^2 + 4a^3 + a^4 + \lambda^2 r^2 (6 - \lambda^2 r^2) - 4\lambda^3 r^3 (1 + \lambda f)}{4(1 + a)^3 \lambda T} + (1 + a)^3 (T/T_0)^\alpha, \quad (3)$$

with $a \equiv \lambda(f + r)$ ¹⁰; the PSD assumes the form

$$S(\omega) \approx \lambda \left[\frac{1 + \lambda^2 r^2}{(1 + a)^3} + (\omega/\omega_0)^{-\alpha} \right] \quad (4)$$

for equilibrium counting in the range $\omega \ll 1/f, 1/r$ ¹⁰.

Figure 2 provides estimated averaged Allan Factors from a typical simulated FGNDP with $\alpha = 0.5$, both with and without refractoriness (solid curves). Also shown are fits from Eq. 1 for the upper curve, and for the full RM-FGNDP (Eq. 3) model for the lower curve (dashed curves). Both theoretical results match their respective simulations extremely well, particularly at the longer counting times which prove most important in estimating α .

Table I shows the results from a number of simulations at different design values of the fractal exponent α . These results are estimated from the simple FGNDP model of Eq. 1 (fourth column), and for the full RM-FGNDP model with refractoriness of Eq. 3 (third column). The RM-FGNDP model yields a much more reliable estimate of α . Similar improvement obtains for the PSD when employing the RM-FGNDP model¹⁰.

Returning to auditory-nerve data, in Fig. 3 we present AF curves for two stimulus levels: spontaneous firing (no stimulus) as shown in Fig. 1, and +40 db:re threshold at CF. Also shown are the predictions of Eq. 3, obtained from a least-squares fit of the logarithm of the AFs. For the upper and lower experimental data curves, the estimated fractal exponents of these firing patterns

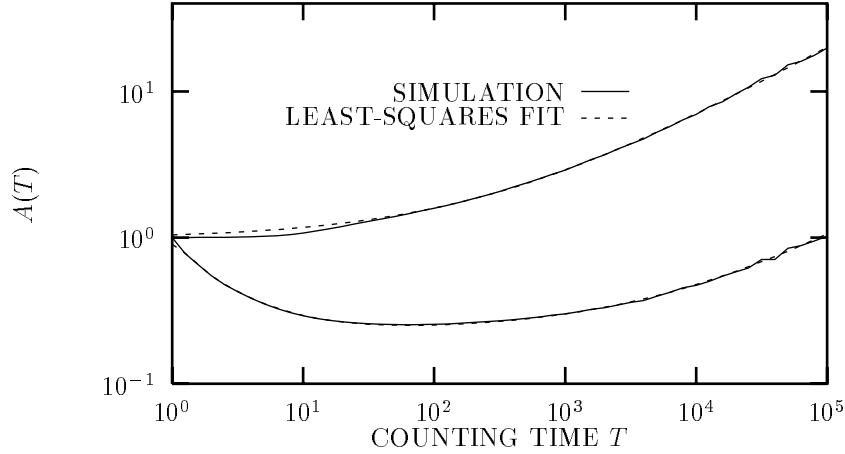


Figure 2: Doubly logarithmic plot of the averaged Allan factor (AF) for simulations of the RM-FGNDP process, with $\lambda = 1$, $\alpha = 0.5$, and $N = 100$ simulations. Upper curves: $f = r = 0$ for simulation (solid curve) and fit from Eq. 1 (dashed curve). Lower curves: $f = r = 1$ for simulation (solid curve) and fit from Eq. 3 (dashed curve).

are $\alpha = 0.71$ and $\alpha = 1.5$, respectively. These are indeed substantially larger than the values $\alpha = 0.48$ $\alpha = 0.96$ obtained without taking refractoriness into account⁹. Within limits imposed by a finite data size, predictions of the RM-

SIMULATION		ESTIMATION	
Fractal Exp.	Refract.	Eq. 3 Bias	Eq. 1 Bias
$\alpha = 0.5$	none	-0.002	-0.046
$\alpha = 0.5$	$f = r = 1$	+0.016	-0.156
$\alpha = 1.0$	none	-0.012	-0.027
$\alpha = 1.0$	$f = r = 1$	-0.015	-0.058
$\alpha = 1.5$	none	-0.019	-0.035
$\alpha = 1.5$	$f = r = 1$	-0.027	-0.090

Table 1: Bias in estimates of the fractal exponent α obtained from the averaged Allan factor (AF) for simulations of the RM-FGNDP process. For all table entries, $\lambda = 1$ and $N = 100$ simulations. Results are reported for three values of α (0.5, 1.0, and 1.5), both with ($f = r = 1$) and without ($f = r = 0$) refractoriness. Bias is calculated by a least-squares fit of the logarithm of the averaged simulated AF plots to the logarithm of Eq. 3, for ten values of the counting time T per decade in the range $10^3 \leq T \leq 10^5$ (left bias column); and to Eq. 1 in the range $10^4 \leq T \leq 10^5$ (right column).

FGNDP model closely follow the AF for the experimental data over all time scales. The PSD predicted by the RM-FGNDP model also accords with that of the data over all frequency scales, as do all other statistics examined to date.

Finally, a similar process, based on a gamma renewal process instead of a Poisson substrate, appears to provide an excellent fit to data collected from neurons in the visual system of the cat, using these same statistics¹⁹. Thus theoretical results obtained for this process will likely provide a superior method for estimating the fractal exponent of these neurons.

3 Conclusion

Over all time scales, analytical predictions of the refractoriness-modified fractal-Gaussian-noise-driven Poisson point process model, with fixed and stochastic refractory periods together, match statistics of experimental data collected from cat auditory-nerve fibers, and of computer simulations of this process. This model therefore provides the best method known to date for estimating the fractal exponent α of neural recordings.

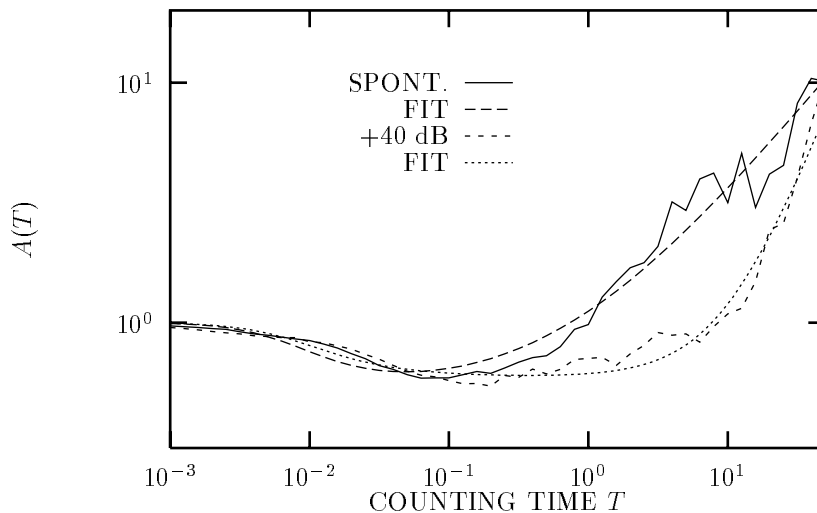


Figure 3: Doubly logarithmic plot of the Allan factor (AF) plot for auditory data (unit L-19, with CF = 3926 Hz, threshold = 19.3 dB SPL, and spontaneous firing rate = 75 spikes/sec.). Upper curves: spontaneous firing conditions (solid curve) and analytical fit from Eq. 3 (long-dashed curve). Lower curves: stimulus applied at CF at +40 dB:re threshold (short-dashed curve) and analytical fit from Eq. 3 (dotted curve).

Acknowledgments

Supported by the Whitaker Foundation under Grant No. CU01455801 and by the Office of Naval Research under Grant No. N00014-92-J-1251.

References

1. Feurstein, M. *et al.*, in preparation.
2. Kelly, O.E. *et al.* (1996), *J. Acoust. Soc. Am.* **99** 2210-2220.
3. Kiang, N.Y-S. *et al.* (1965), *Discharge Patterns of Single Fibers in the Cat's Auditory Nerve*, Res. Monogr. No. 35 (MIT, Cambridge, MA).
4. Kumar, A.R. and Johnson, D.H. (1993), *J. Acoust. Soc. Am.* **93** 3365.
5. Lowen, S.B. and Teich, M.C. (1991), *Phys. Rev. A* **43** 4192-4215.
6. Lowen, S.B. and Teich, M.C. (1993), *Phys. Rev. E* **47** 992-1001.
7. Lowen, S.B. and Teich, M.C. (1995), *Fractals* **3** 183-210.
8. Lowen, S.B. and Teich, M.C. (1996). in *Computational Neuroscience*, ed J.M. Bower (Academic, New York), pp. 447-452.
9. Lowen, S.B. and Teich, M.C. (1996), *J. Acoust. Soc. Am.* **99** 3585-3591.
10. Lowen, S.B. (1996), *CTR Technical Report 449-96-15* (Columbia Univ., New York).
11. B.B. Mandelbrot (1983), *The Fractal Geometry of Nature* (Freeman, New York).
12. Müller, J.W. (1974), *Nucl. Inst. Meth.* **117** 401-404.
13. Powers, N.L. and Salvi, R.J. (1992), in *Abstracts of the Fifteenth Midwinter Research Meeting of the Association for Research in Otolaryngology*, ed D.J. Lim (Association for Research in Otolaryngology, Des Moines, IA), Abstract 292, p. 101.
14. Ricciardi, L.M. and Esposito, F. (1966), *Kybernetik* **3** 148-152.
15. Teich, M.C. *et al.* (1978), *J. Opt. Soc. Am.* **68** 386-402.
16. Teich, M.C. (1989), *IEEE Trans. Biomed. Eng.* **36** 150-160.
17. Teich, M.C. (1992), in *Single Neuron Computation*, ed. T. McKenna *et al.* (Academic, Boston), pp. 589-625.
18. Teich, M.C. and Lowen, S.B. (1994), *IEEE Eng. Med. Biol. Mag.* **13** 197-202.
19. Teich, M.C. *et al.* (1996), *J. Opt. Soc. Am.* **A** in press.
20. Young, E.D. and Barta, P.E. (1986), *J. Acoust. Soc. Am.* **79** 426-442.